Chapter 2

Positron flux on the moderator

Positrons from radioactive decay have an energy range of several hundred keV. Therefore, the first step in achieving a high positron trapping rate is to maximize the flux of high-energy positrons onto the positron moderator, where they are slowed to sub-eV energies. Because the Penning trap and moderator are in a high magnetic field (5.9 Tesla), the simplest way would be to mount the positron source very close to the moderator inside the trap's vacuum enclosure and allow the strong magnetic field to guide the positrons to the moderator. Unfortunately, the experimenters must spend a considerable amount of time in close proximity to the trap's vacuum enclosure (hereafter referred to as the "trap can") while they make vacuum seals and test electronics. Therefore, we designed a dewar and support system which can accept the radioactive source and position it *after* the trap can has been sealed, tested, and lowered into the magnet. This minimizes the experimenters' exposure to harmful gamma radiation. The entire apparatus is described in Section 2.2.

Once the radioactive source is properly positioned, positrons follow the strong magnetic field lines, as described in Section 2.3, all the way to the moderator, where their flux can be measured using the lock-in technique described in Section 2.4.

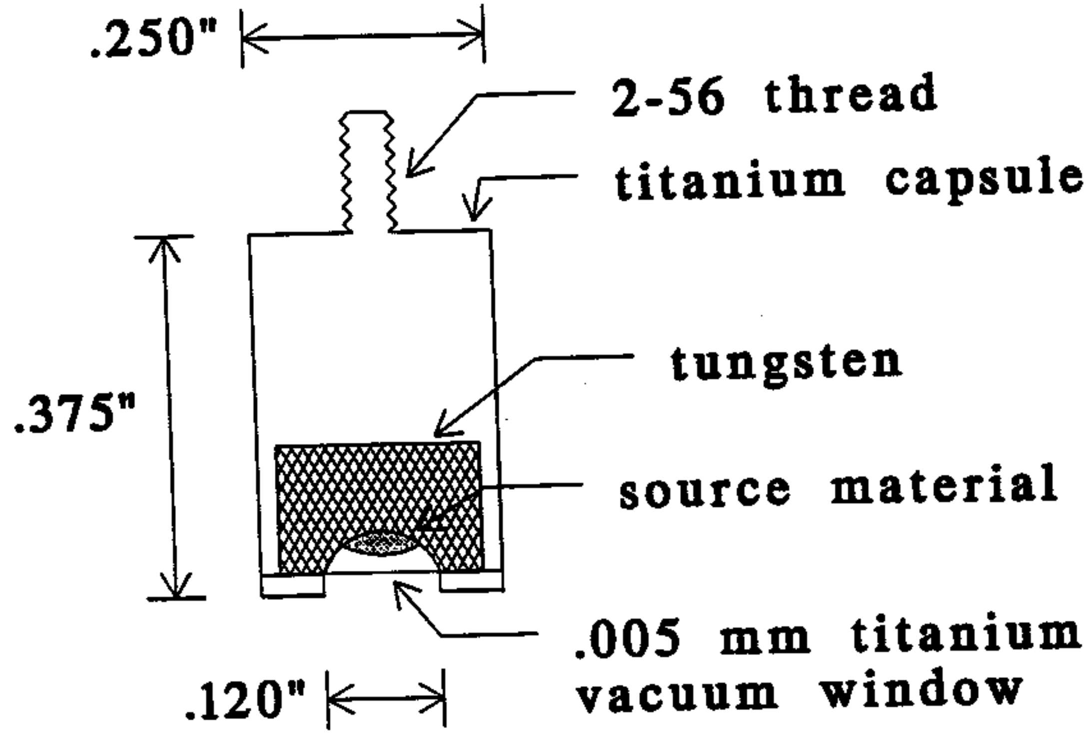

Figure 2.1: Cross section of ^{22}Na positron source capsule.

2.1 The positron source

There are only a few positron-producing radionuclei with half-lives sufficiently long to be useful in this application. The most promising are cobalt-58, which has a half-life of 72 days and a positron efficiency (*i.e.* the fraction of all decays which produce positrons) of 15 percent, and sodium-22, which has a half-life of 2.6 years and a positron efficiency of 90 percent. We also require a source which can safely withstand repeated cycling to high vacuum and liquid helium temperatures.

We contracted with New England Nuclear/Dupont to obtain a 20 milli-Curie ^{22}Na sealed source, pictured in Fig. 2.1. The radioactive material is in the form of a paste which has an active area with a radius $r_s \simeq 1.0$ mm. The capsule

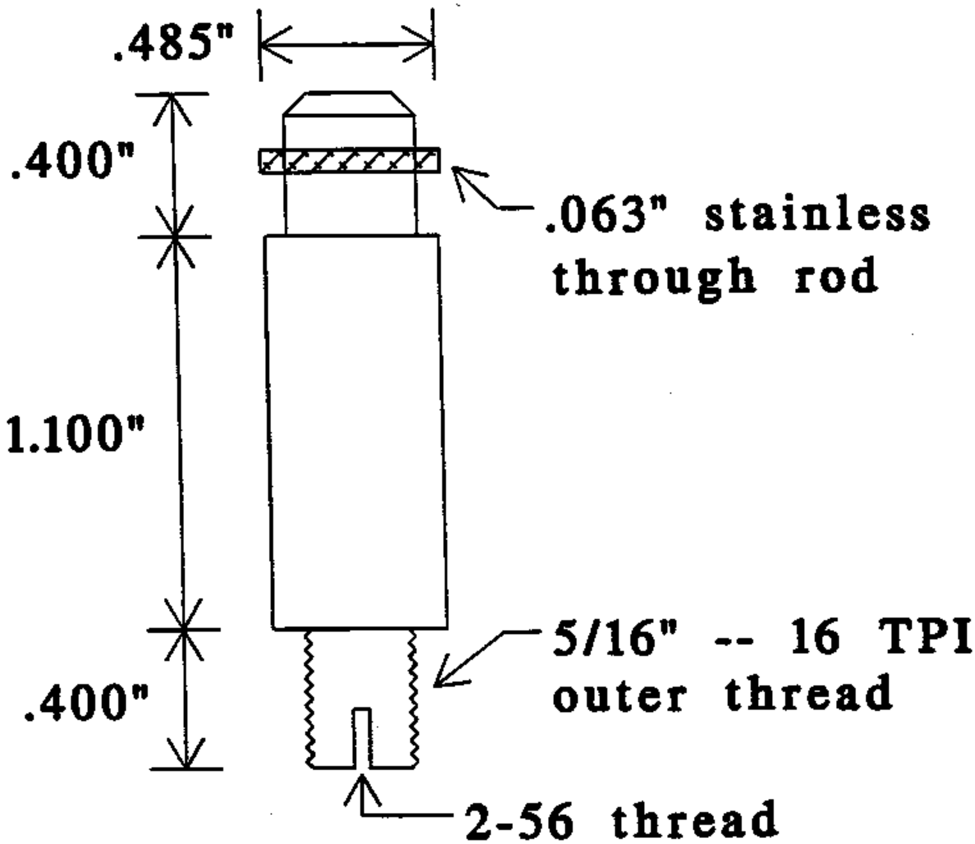

Figure 2.2: Elkonite plug used for loading and unloading the source capsule.

was sealed by electron beam welding a 5 μm titanium window over the mouth of the capsule. A tungsten backing plate increases positron back-scatter towards the window and thereby increases positron emission in the forward direction.

This source capsule is mounted onto the bottom of an Elkonite (90% tungsten, 10% copper) plug, shown in Fig. 2.2. The top of this plug has a 0.063 inch diameter horizontal through rod which allows it to be grasped by a spring-loaded "bayonet socket," shown in Fig. 2.3, at the end of a 1.5 meter rod. The outer threads on the Elkonite plug match threads inside a lead container used to store the source when it is not in use. When the radioactive source capsule was received, it was mounted "by hand" (actually, a pair of ten inch long tongs were used) into the 2-56 inner threads of the Elkonite plug. Thereafter, the source capsule and plug

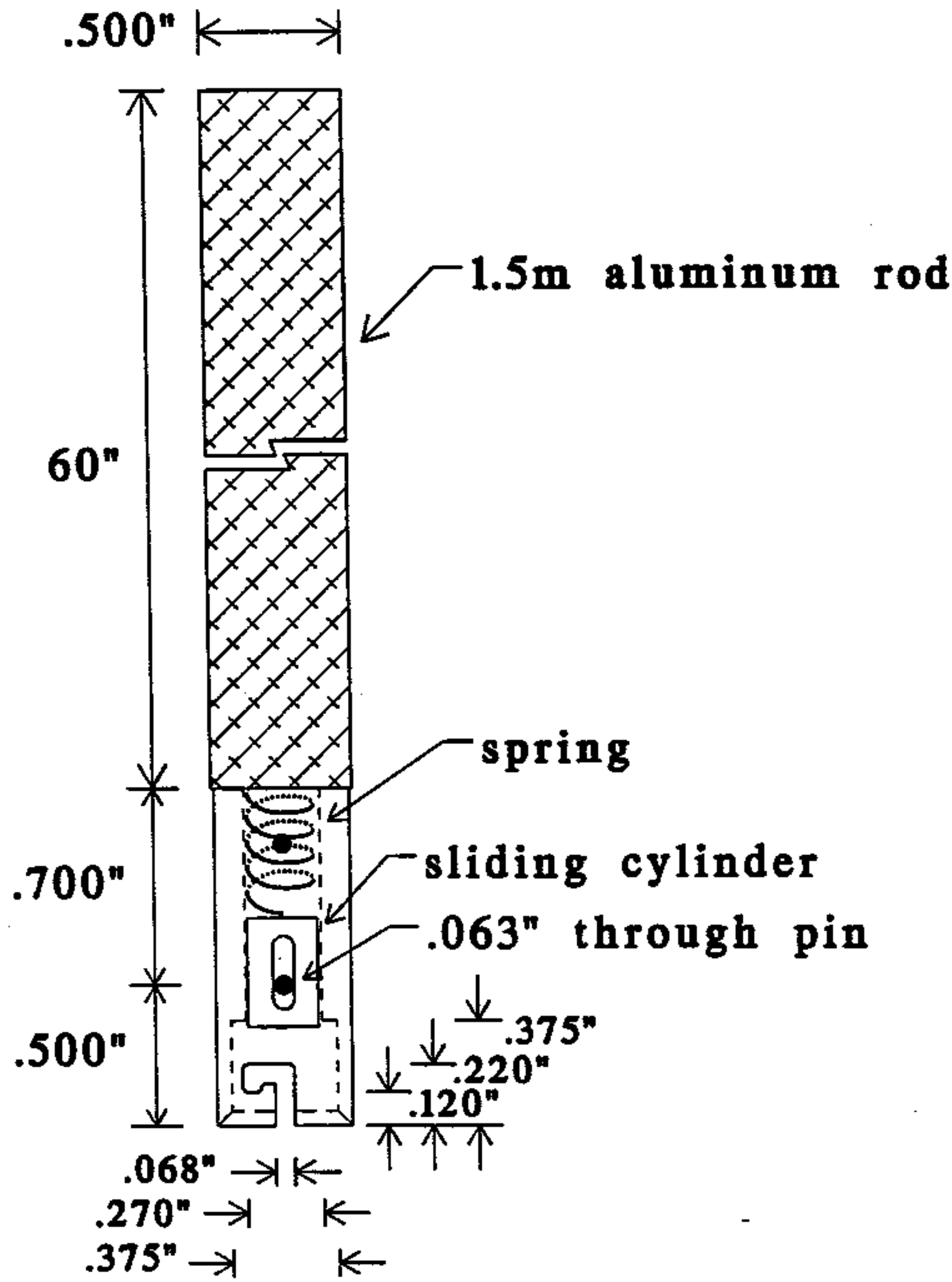

Figure 2.3: "Bayonet socket" attached (with internal spring) to the end of a 1.5 meter rod used for manipulating the source capsule and plug.

were manipulated exclusively by means of the 1.5 meter loading rod.

New England Nuclear estimates that, even if the source material is deposited properly into the capsule, 50% of the positrons emitted in the forward direction (towards the window) are absorbed within the capsule, due to the thickness of the source material. This is consistent with our measurements (Section 2.4). Therefore, increasing the source activity by increasing the source material thickness would cause little increase in positron emission. Increasing the active area of the source material would not increase the flux on the moderator because of beam collimation at the Penning trap entrance apertures (Section 2.3).

2.2 Apparatus design from source to moderator

The liquid helium dewar and overall support system for this positron trap is designed to be highly compatible with the existing apparatus used at CERN to capture and study antiprotons (described in Refs. [23] and [24]). Apart from the actual Penning trap electrodes, the components of the two systems are nearly identical. This will greatly facilitate the next stage of the experiment, when positrons and antiprotons are simultaneously captured in the same vacuum enclosure and merged to form antihydrogen.

2.2.1 Magnet, dewar, support system, and vacuum enclosure

A large-scale picture of the apparatus is given in Fig. 2.4. The superconducting solenoid made by Nalorac Cryogenics can produce a 5.9 Tesla field which is uniform to within one part in 10^8 over a volume of approximately 1 cm^3—roughly the volume of the interior of the Penning trap. The inner bore of the magnet's dewar has a diameter of 4 inches, and can be cooled via a connection to a liquid nitrogen reservoir. The Penning trap's support apparatus and vacuum enclosure

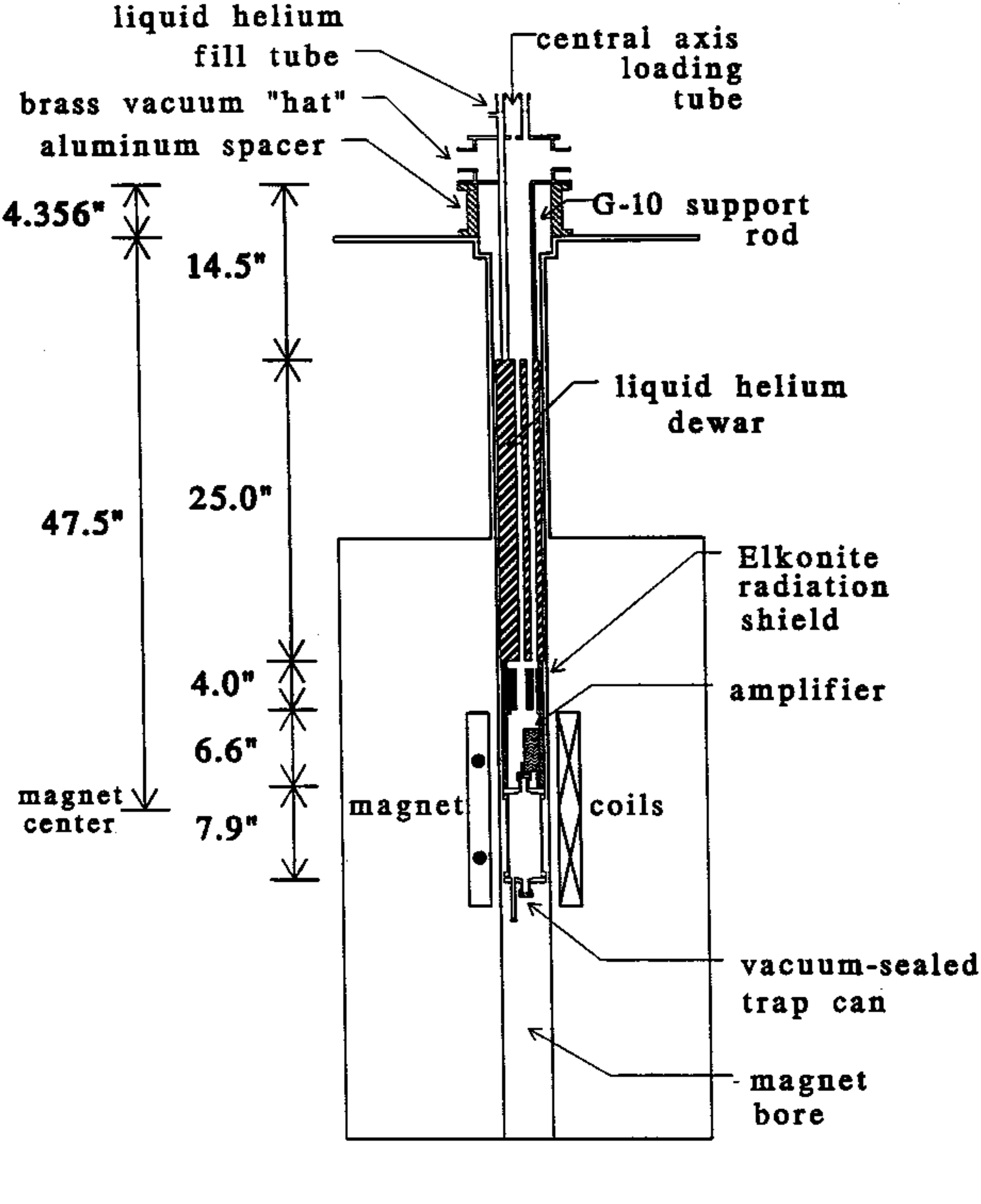

Figure 2.4: Scaled picture of superconducting magnet, liquid helium dewar, and support system for the positron trap.

have outer diameters of 3.5 inches or less so that they can easily be inserted into and withdrawn from the magnet bore. The magnet bore is evacuated to less than 10^{-6} Torr during normal operation.

The positron trapping apparatus has a liquid helium dewar, separate from the magnet's dewar, which has a volume of about 2.3 liters and a hold time of three days when the magnet's inner bore is evacuated and a thermal radiation shield (thermally connected to the cold helium exhaust gas) is installed between the dewar and the magnet bore wall. This helium dewar also has a 0.5 inch diameter tube down its center, through the entire length, which allows us to insert and extract the radioactive source without removing the apparatus from the magnet bore.

A 3.5 inch diameter Elkonite (90% tungsten, 10% copper) shield is bolted onto the bottom of the trap's liquid helium dewar. Approximately 0.8 inches was bored out of its center, and the radioactive source normally resides in the center of this shield, as is shown in Fig. 2.5. Elkonite has a density of about 19 g/cm^3, so this provides most of the gamma ray shielding required to protect the experimenters during normal operation. Care had to be taken in the choice of material, since some commercially available "heavy metal" materials are sintered and contain copper-nickel alloys which could undergo a ferromagnetic transition at temperatures between 77 K and 4 K [25], which would have been disastrous. With the additional shielding provided by the magnet itself, two inches of lead stacked onto the upper shoulder of the magnet dewar, a quarter inch of lead wrapped around the upper neck of the magnet, and eight inches of concrete stacked around the side of the magnet, the gamma radiation produced by the 20 mCi source is reduced to one or two times natural background measured outside the shielding.

A 7 inch long copper stand is bolted to the bottom of the Elkonite shield. This region between the Elkonite and the trap can allows easy access to the electrical feedthroughs on the top of the trap can. It provides space for the sensitive amplifier circuit described in Chapter 5 as well as other electronic components (low-pass

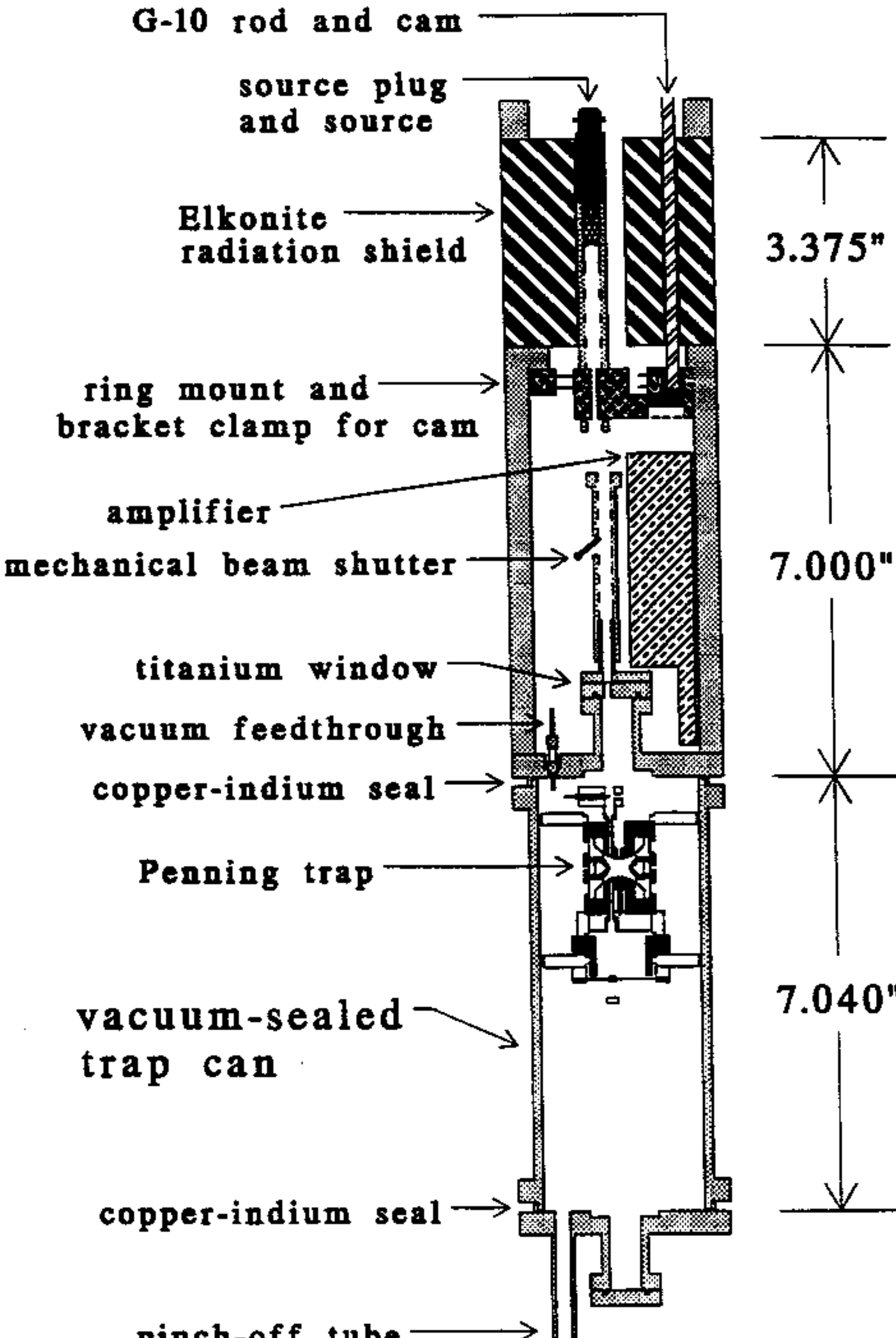

Figure 2.5: Close-up picture of the vacuum-sealed trap can, stand, and Elkonite radiation shield. The positions of the radioactive source and the Penning trap are also shown.

filters, etc.), and for the positron source positioner described in Section 2.2.2.

The Penning trap is contained a separate vacuum enclosure, the "trap can." After the Penning trap is assembled, the trap can is sealed with compressed indium o-rings located between the copper components of the trap can. It is evacuated at room temperature to about 10^{-7} Torr through a pinch-off tube, then sealed. When the apparatus is lowered into the magnet bore and the trap can is cooled to 4 K by thermal contact to the liquid helium dewar, the pressure inside the can drops to levels suitable for long-term storage of antimatter, a pressure below 5×10^{-17} Torr having been observed [15]. Energetic positrons from the ^{22}Na source enter the trap can through a 5 μm titanium window, which is held in place by another indium compression seal, as shown in Fig. 2.5.

The overall apparatus is designed so that, after thermal contraction following cooldown to liquid helium temperatures, the center of the Penning trap is located in the center of the magnetic field. Construction materials such as OFE copper were chosen with as small a magnetic susceptibility as possible in order to minimize field inhomogeneities.

2.2.2 Positioning the radioactive source

The radioactive source is inserted and removed along the central symmetry axis of the trap's helium dewar, which is also the central symmetry axis of the Penning trap. However, positrons must ultimately enter the Penning trap *off* its central symmetry axis (Chapter 4). Moreover, while the Penning trap is located in the center of the superconducting magnet's field, the positron source is located in the magnet's fringing field. It is therefore necessary to move the source radially across the magnetic field lines (from right to left in Fig. 2.5 and 2.6) after the source has been inserted so that the positrons travel along the curving magnetic field lines to the moderator. Figure 2.6 shows an exaggerated view of the magnetic field lines superimposed on the positron source, Penning trap, and moderator.

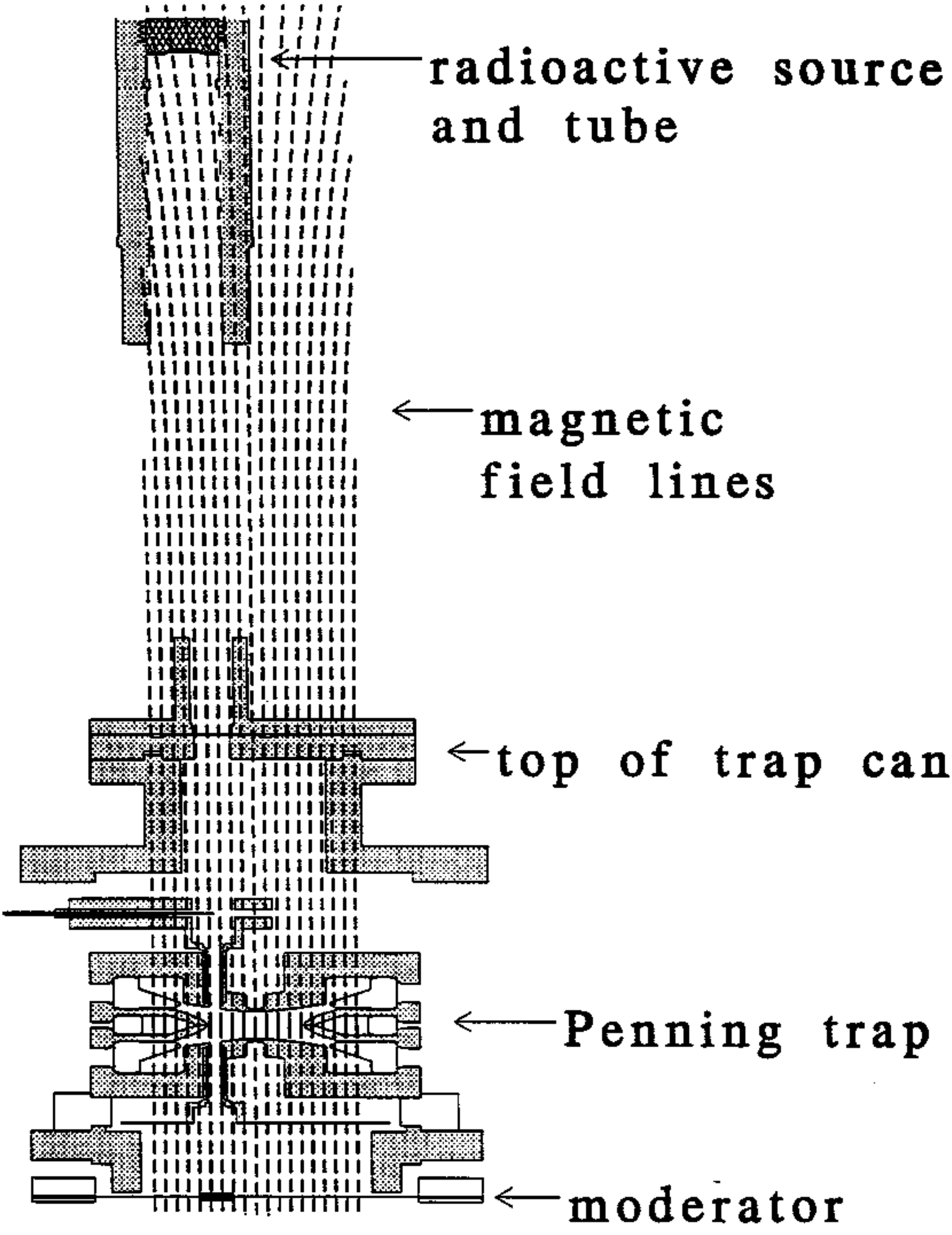

Figure 2.6: Positron source, Penning trap, and moderator. Curving magnetic field lines from the superconducting solenoid are superimposed. The horizontal scale is expanded by a factor of 3 compared to the vertical scale.

Angular alignment of the source with the small entrance holes into the trap relies on careful alignment during trap assembly. The radial adjustment of the source is accomplished by using the cam-and-shaft device (Fig. 2.7) which is mounted immediately below the Elkonite shield; it functions even when the magnet bore is evacuated and at liquid helium temperatures. The Elkonite source plug and the radioactive source are mounted via the 1.5 meter "bayonet" rod into the moving source holder, which is in turn held by the bracket clamp. When the cam rotates, the bracket clamp slides along rods which are held in place by the ring clamp. The cam consists of a 0.55 inch diameter copper disk mounted 0.125 inches off-center from the cam's central axis. A long (thermally insulating) rod made from G-10 (epoxy fiberglass) extends from the cam, through another clearance tube in the helium dewar (located 1 inch off the central symmetry axis) to a motional vacuum feedthrough in the magnet's brass "hat." As the cam rotates, the bracket clamp, source holder, and source move radially in the magnetic field.

Figure 2.9 shows a typical example of the positron flux on the moderator (and also the positron loading rate into the trap) as a function of the cam angle. In one position, chosen to be 0°, the source is located along the central symmetry axis of the dewar and trap. As the cam rotates through 180°, the source moves radially across the magnetic field lines $\sim$ 9 mm. When the source is located $\sim$ 6.6 mm off of the symmetry axis, corresponding to a cam position of 70°, it is in the proper position for positrons to follow the magnetic field lines all the way to the moderator. As the cam continues from 180° to 360° the source moves back to the central axis; therefore, there are two positions in angle which maximize the flux of positrons incident on the moderator.

The entire apparatus was carefully shimmed so that it hung true to vertical, from the brass hat to the bottom of the trap can, to within 0.02°. Even so, because the superconducting solenoid is not properly aligned with its own dewar, we found it necessary to rotate the entire apparatus within the magnet's bore, with certain orientations resulting in no positrons hitting the moderator.

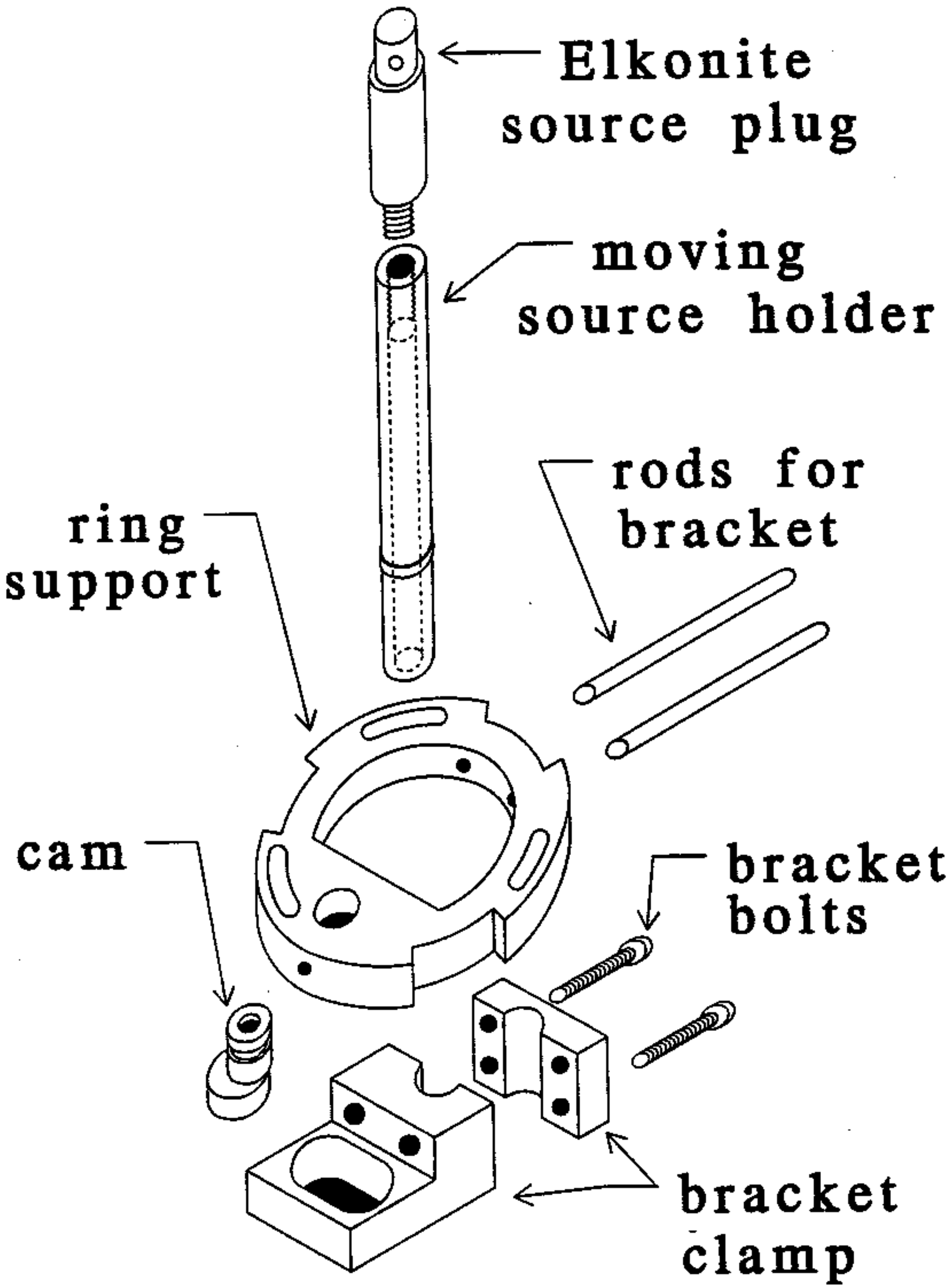

Figure 2.7: Three-dimensional view of the components of the cam-and-shaft device used to hold and position the radioactive source. The cam is held in the ring support by a set screw. As the cam rotates, the bracket clamp and source holder slide along the rods.

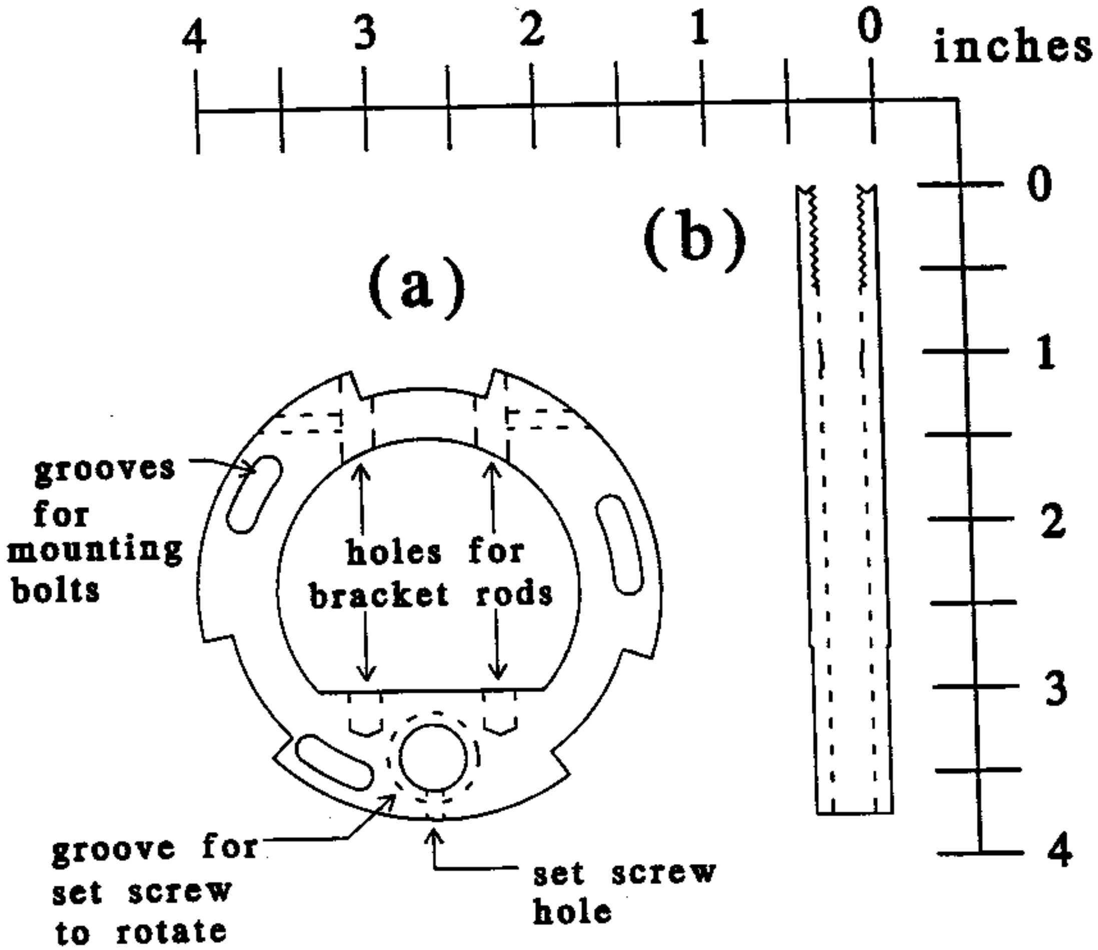

Figure 2.8: Cross-sectional view of (a) the ring clamp, and (b) the moving source holder.

In order to measure the flux of positrons on the moderator, we found it necessary to install a beam shutter between the positron source and the trap can, as shown in Fig. 2.5. This was achieved by attaching a small loop of wire to a flap of non-conductive material (G-10 in this case) thick enough to stop the positrons. Just as in an ordinary current meter, a small electric current through the loop causes it to feel a strong force due to the large magnetic field from the solenoid. The flap and coil are mounted on a hinge so that the flap pivots to block the

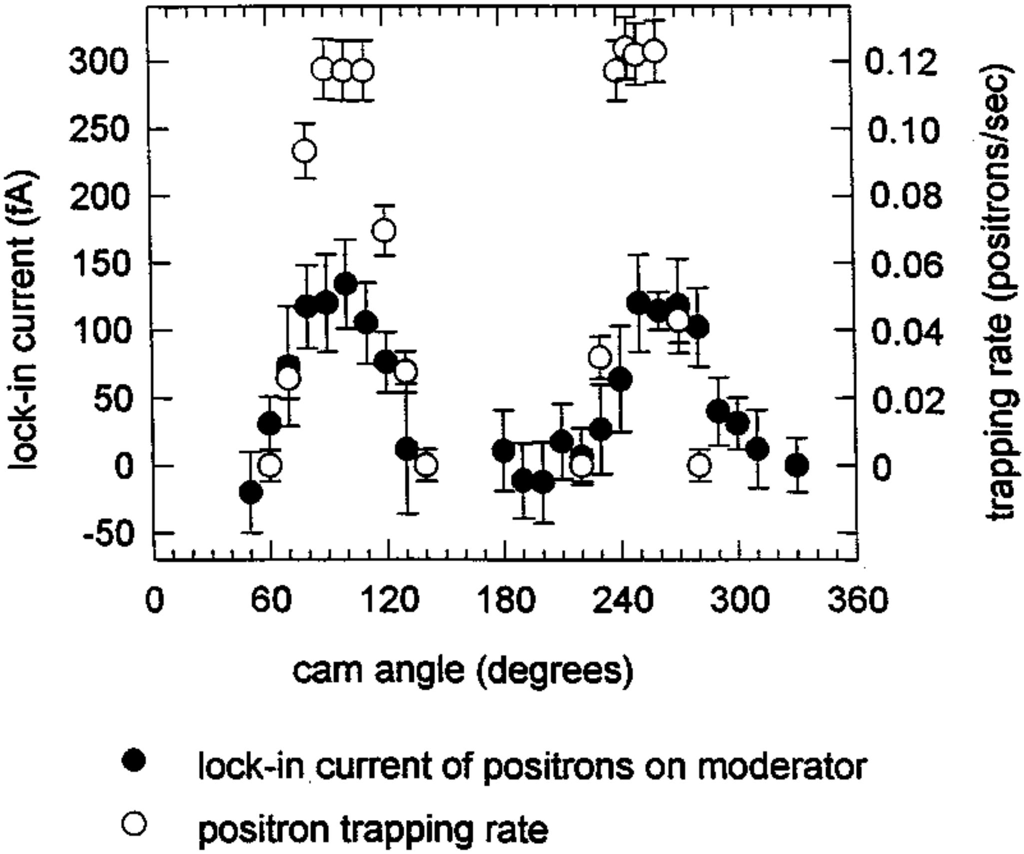

Figure 2.9: The positron trapping rate o, and the measured current of the lock-in detector • due to positron flux on the moderator, as a function of cam angle. The actual positron current into the moderator is 3 to 4 times the measured lock-in value.

positron beam when current flows in one direction, while allowing the positrons to pass when the current is turned off (or made to flow in the opposite direction).

2.2.3 Penning trap and moderator

The Penning trap is pictured in Fig. 2.10. It is very similar in design to Penning traps used for high precision measurements on electrons [22,26,27]. The endcap and ring electrodes are made from OFHC copper; their inner surfaces are machined

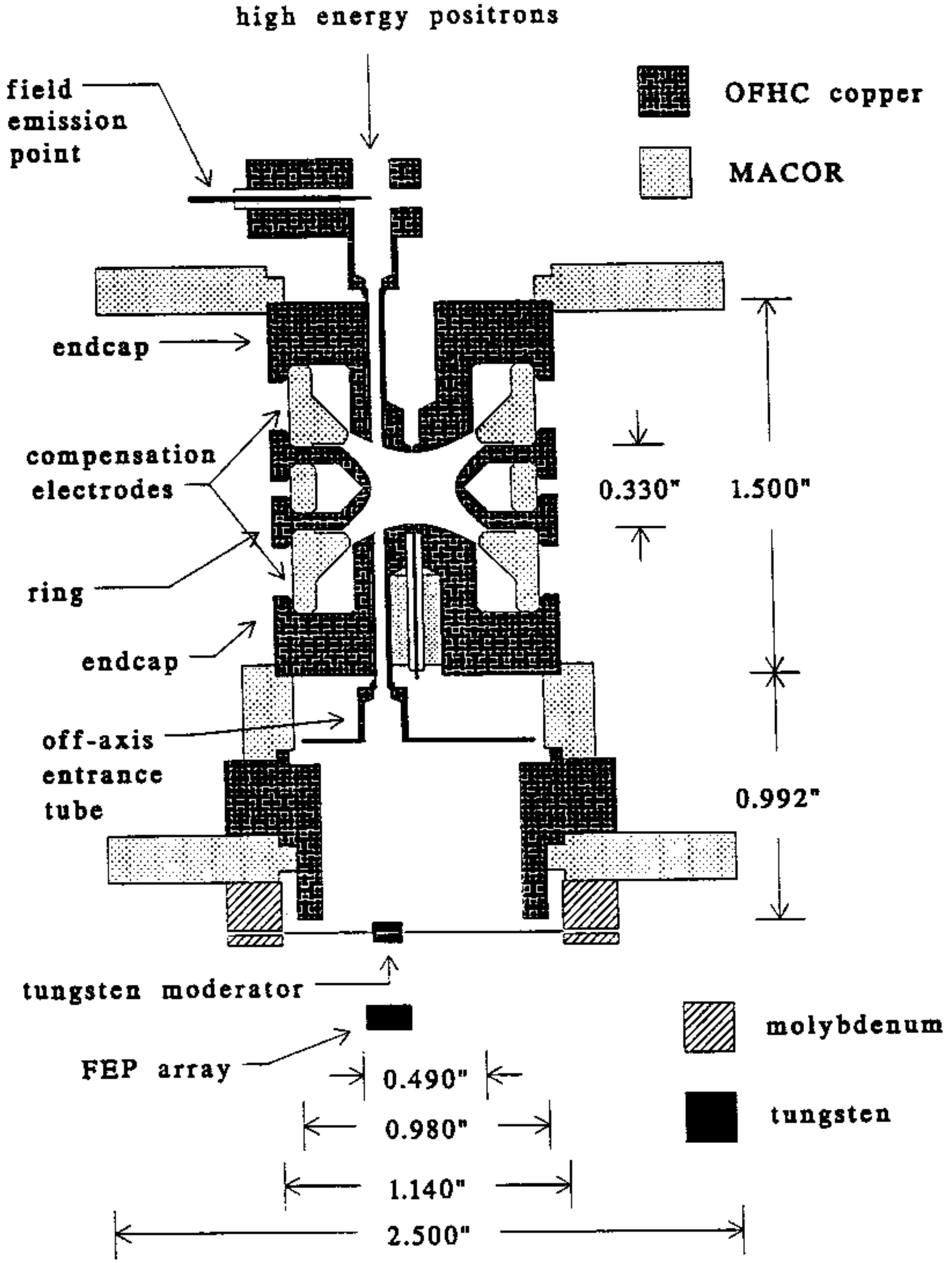

Figure 2.10: Cross section of Penning trap and moderator used for continuous loading of positrons. The entrance tubes are located 0.14 inches from the trap's central symmetry axis.

along hyperbola of revolution around the $\hat{z}$ axis. This hyperbolic geometry insures that the electric potential experienced by the positrons during their first orbits inside the trap volume—when they are still energetic and travel very near to the inner surfaces of the electrodes—is as nearly as possible a pure quadrupole. Other possible electrode geometries (*e.g.* cylindrical) create electrostatic potentials which depart significantly from a quadrupole near the electrode surfaces. The resistive circuit we use to extract energy from the positrons (described in Section 5.1) works most efficiently when the positrons experience a purely quadrupole potential throughout their entire motion (Section 4.3).

The inner surfaces of the endcap and ring electrodes are coated with a thin layer of Aquadag (graphite) to reduce electric field inhomogeneities due to patch effects. The diameter of the ring electrode is $\rho_0 = 0.168$ inches, and the distance between the two endcap electrodes at closest approach is $2z_0 = 0.288$ inches. The endcap electrodes have small holes (0.5 mm diameter) through their centers. Field emission points mounted in these apertures allow us to directly load electrons into the center of the trap. The off-axis apertures in the endcap electrodes are located $\rho_h = 0.140$ inches from the central axis. The apertures themselves have a diameter of 1.0 mm, although the holes drilled into the electrodes have a 2.0 mm diameter which only narrows to 1.0 mm within the last millimeter before the inner surface.

The compensation electrodes are made of MACOR (a machineable ceramic). Their surfaces near the trap's center are plated with copper so that particles inside the trap do not have a direct line-of-sight to a nonconductive surface. The copper plating on the bottom compensation electrode is split into four quadrants to allow for magnetron sideband cooling of the positrons (Section 5.3). The purpose of compensation electrodes is to allow an additional degree of control over the shape of the electrostatic potential inside the trap. Inevitably, the potential provided by the ring and endcap electrodes is not purely quadrupole due to machining uncertainties and truncation of the electrodes. The adjustable voltage applied to the compensation electrodes gives an extra degree of freedom with which to correct some of those errors.

The entrance tubes are made of OFHC copper with a diameter of $\sim$ 1.4 mm and a wall thickness of just a few tens of microns. They are insulated from the endcap electrodes by thin alumina sleeves.

A field emission point (FEP) is made by electrochemically etching the tip of a 0.5 mm diameter tungsten rod to a sharp point. Biasing the point to a few hundred volts results in an electron emission current which ranges from a few picoamps to hundreds of nanoamps. In addition to the one mounted in the center of the bottom endcap electrode, another FEP is mounted in the horizontal section of the upper entrance tube, with its tip located directly over the endcap's off-axis aperture. This is an important diagnostic feature since it allows us to easily load electrons in the same off-axis position as the positrons are initially loaded.

The moderator is a single tungsten crystal 0.08 inches thick and 0.12 inches in diameter with its surface along the (110) crystal plane. Two small holes were drilled through its side (taking care not to mar the crystal surface) with an EDM machine. It is mounted with the crystal surface perpendicular to the magnetic field lines via 0.07 mm diameter tungsten wires strung through the holes, connecting it to a molybdenum ring. The moderator is mounted in this fashion to allow it to be heated in thermal isolation from the rest of the trap via electron bombardment from the field emission point array. The field emission point array, described in more detail in Section 3.3, is mounted directly below the moderator. Naturally, great care was taken to align the loading tubes with each other, the moderator, and the thin titanium vacuum window.

2.3 Calculated positron flux on the moderator

The expected positron flux on the moderator is determined by the activity of the source, the fraction of positrons which successfully traverse the fringing magnetic field, and the fraction of these which make it through the small apertures in the endcap electrodes. During most of the measurements reported here the source was at 10 mCi. Only 90% of the decays produce positrons, only half of which travel in the forward direction towards the source window. Factoring in the additional 50% self-absorption of forward-emitted positrons within the source capsule itself, this yields a total source activity $A = 8.3 \times 10^7$ positrons per second.

Fermi's theory of beta decay [28] gives the positron energy spectrum

$$\begin{aligned} N(\gamma) &= CF_+(Z,\gamma)\gamma(\gamma_e - \gamma)^2(\gamma^2 - 1)^{1/2} \\ F_+(Z,\gamma) &= \frac{-2\pi Z\alpha(1-\gamma^{-2})^{-1/2}}{1-\exp(2\pi Z\alpha(1-\gamma^{-2})^{-1/2})} \end{aligned} \tag{2.1}$$

where γ is the usual relativistic energy factor, $N(\gamma)$ is the differential probability that a positron has energy γ, C is a normalization constant, γ_e is the endpoint energy of the beta decay spectrum, Z is the atomic number of the final state, α is the fine structure constant, and $F_+(Z,\gamma)$ is the Fermi function for positive charges, which includes the effects of the Coulomb interaction between the positron and the nucleus. The source material, and the thin window which seals the source capsule, moderate and shift this energy spectrum slightly, but the effect is small enough to be unimportant for these calculations. (See for example Ref. [1] pages 21–25 and also Ref. [29].) The pressure in the magnet bore is kept below 10^{-6} Torr and therefore has no effect on the positrons.

The strong magnetic field controls the trajectory of the positrons so that they essentially travel along the field lines while executing cyclotron motion. The cyclotron motion radius is given (in S.I. units) by

$$r_c = \frac{mc}{eB}(\gamma^2 - 1)^{1/2}\sin\theta \tag{2.2}$$

where m is the positron mass, e the electric charge, c the speed of light, B the magnetic field strength, and the positron is emitted at angle θ with respect to the magnetic field lines. We use Eq. 2.1 and the assumption of isotropic emission to calculate the expected distribution of cyclotron radii for a ^{22}Na source, shown in Fig. 2.11. We expect that positrons do not emerge exactly isotropically from the source capsule, since those emitted at large angles with respect to the magnetic field lines are preferentially absorbed within the capsule. This has the effect of reducing the large-radius tail of the distribution.

Because the cyclotron frequency

$$\nu_c = \frac{eB}{2\pi\gamma m} \tag{2.3}$$

is so rapid (ν_c = 165 GHz when B = 5.9 Tesla and γ = 1), the magnetic field which the positrons experience changes very little in the course of one cyclotron orbit, even at these relativistic energies. This makes calculation of the positron trajectories much easier insofar as the ratio of the cyclotron energy and magnetic field strength is an adiabatic invariant. Two important effects are noted. First, the active area of the positron beam—which initially has $r_s \simeq 1.0$ mm—shrinks by B_s/B_t, where $B_s = 1.9$ Tesla is the field strength at the source and $B_t = 5.9$ Tesla is the field strength at the trap. Second, kinetic energy in the positrons' cyclotron motion increases by a factor of B_t/B_s. This additional cyclotron energy must be taken out of their "axial" kinetic energy (*i.e.* parallel to the magnetic field lines). Positrons emitted at a forward angle greater than a "critical" angle, given by

$$\sin\theta_c = \sqrt{B_s/B_t}, \tag{2.4}$$

thus do not have sufficient axial energy to reach the moderator. They magnetically "bounce" off of the compressing magnetic field lines and return to the source. After this magnetic compression the total positron beam flux is reduced by a factor of $(1 - \cos\theta_c)$. The calculated distribution of cyclotron radii after magnetic compression is shown in Figure 2.11.

The final loss of positron flux occurs because the active area of the beam is larger than the effective aperture size in the endcap electrodes. The off-axis holes in the endcaps have radius r_h = 0.5 mm. Positrons with large cyclotron radii

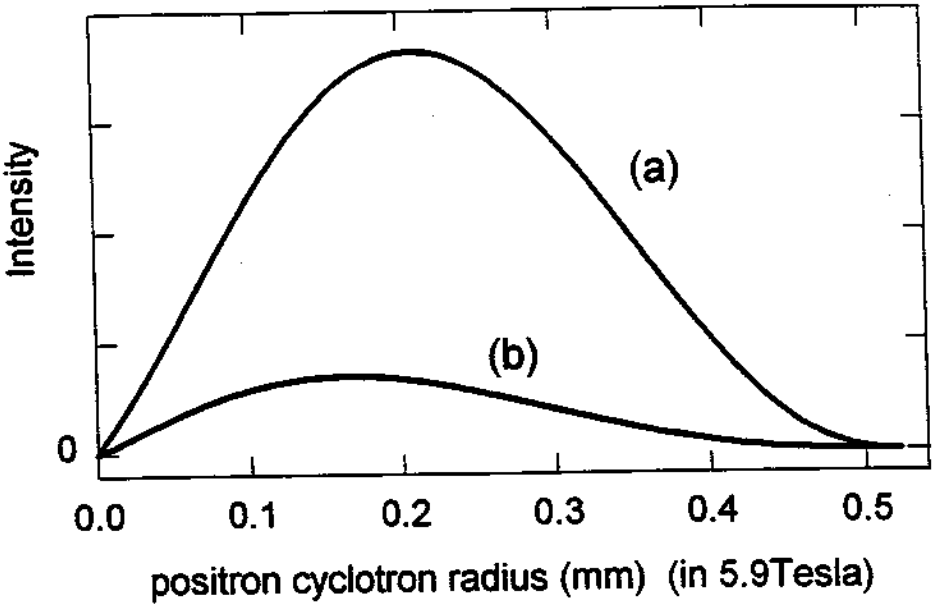

Figure 2.11: Sodium-22 positron cyclotron radii distribution in a $B_t = 5.9$ Tesla field, (a) without magnetic compression, area normalized to 1. (b) with magnetic compression after emission in $B_s = 1.9$ Tesla, area normalized to $(1 - \cos\theta_c)$.

traveling near the edges of the hole impact the sides of the aperture and are lost. The effective aperture radius for these energetic positrons is therefore reduced by their average cyclotron radius from r_h to $r_e \approx 0.27$ mm. and the flux is reduced by a factor of

$$\frac{\text{Effective area of holes}}{\text{Active area of beam after magnetic compression}} = \frac{\pi r_e^2}{\pi r_s^2(B_s/B_t)}. \tag{2.5}$$

Combining the factors of magnetic bouncing and beam collimation at the apertures yields a total expected flux on the moderator

$$F = A\frac{r_e^2}{r_s^2}\frac{B_t}{B_s}\left[1 - \sqrt{\left(1 - \frac{B_s}{B_t}\right)}\right] \approx 3 \times 10^6 \text{ e}^+/\text{s}. \tag{2.6}$$

The flux can be calculated more carefully by integrating the "effective aperture radius" over the distribution of cyclotron radii given in Fig. 2.11, and this gives nearly the same result as Eq. 2.6 using $r_e \approx 0.27$ mm.

2.4 Measuring the positron flux

The flux of positrons into the moderator given in Eq. 2.6 corresponds to a continuous electrical current of 480 fA. We were able to measure this by connecting the moderator directly to the small-current input of a lock-in amplifier and driving the mechanical beam shutter at 1 Hz. This is an important diagnostic tool because it allows us to test the apparatus alignment and to maximize the positron flux without relying on any knowledge of the moderator's condition or the trapping efficiency.

In order to average out the 1 Hz steps, and to obtain an accurate measurement with a signal greater than the Johnson noise, it was necessary to use a lock-in integration time constant of at least 10 seconds. It was also necessary to rotate the cam back and forth (between the "beam on" and "beam off" positions) many times, subtracting the values of neighboring measurements, to eliminate long-term drifts in the signal.

Another possible concern in this measurement was the slow, secondary electrons (typically of a few eV in energy) released when positrons impact a surface. Secondary electrons knocked free from the high vacuum side of the trap can's thin titanium window and from the entrance hole boundaries travel with the positrons to the moderator, where they cause a systematic underestimation of the positron flux. Conversely, electrons released from the moderator by the positrons' impact cause a systematic overestimation of the flux. To eliminate both these concerns, the bottom entrance tube was kept at –50 Volts during this procedure. This is sufficient to reflect most secondary electrons from *either* direction. (The tube bias was reversed once every minute—for one second—to drive out any charged particles which might have accumulated in the region.)

The lock-in amplifier routinely measured a difference of 120 ± 20 fA between the "beam on" and "beam off" cam positions. Unfortunately, we do not know the exact shape of the input signal produced as the beam shutter chops the positron beam. The lock-in amplifier operates by mixing the input signal (in this case, whatever lineshape is produced by the beam chopping) with a reference signal (in this case, a sine wave which was also used to drive the beam shutter) and gives the d.c. component. We tested the lock-in amplifier and found that when the reference input was given a sine wave and the input signal was a sine wave of the same frequency, the conversion factor from peak-to-peak to d.c. current was 0.33. When the input signal was a triangle wave, the conversion factor was 0.25. Therefore we conclude that the measured lock-in signal of 120 fA corresponds to a continuous positron beam current between 350 and 480 fA, which is consistent with the expectations outlined in Section 2.3.